

AD-A233 932

Mass Spectral Fragmentation Pathways of  
*N*-Acetylnitramines:1-Acetylhexahydro-3,5-dinitro-1,3,5-triazine and  
1-Acetyloctahydro-3,5,7-trinitro-1,3,5,7-tetrazocine② DTIC  
ELECTE  
MAR 2 9 1991  
S G

Elizabeth P. Burrows

US Army Biomedical Research and Development Laboratory, Fort Detrick, Frederick, MD 21702-5010, USA

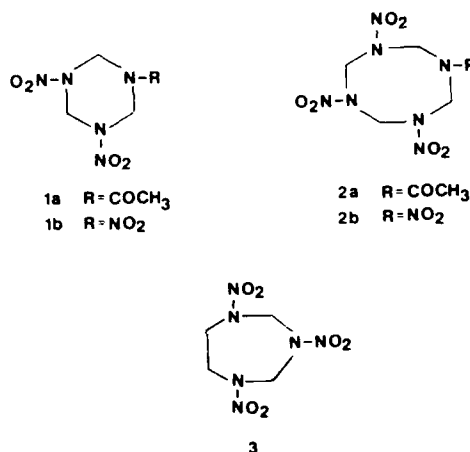
Mass spectra of the *N*-acetylnitramines 1-acetylhexahydro-3,5-dinitro-1,3,5-triazine (TAX) and 1-acetyloctahydro-3,5,7-trinitro-1,3,5,7-tetrazocine (SEX) were recorded in electron impact (EI) and positive and negative chemical ionization (PCI and NCI) modes, and the fragmentation pathways were compared with those of other nitramines which have been well documented and characterized. Unexpectedly, for both acetylnitramines in the EI mode (and in the PCI mode) proton adducts were the only molecular ion species observed; in neither mode was there evidence for higher adducts. In contrast, for TAX in the NCI mode the  $[M + NO_2]^-$  adduct was the second most abundant ion (70%); relatively small amounts of the  $[M + NO]^-$  adduct (2%) and the hydrogen adduct  $[MH]^-$  (3%) were observed. Under identical NCI conditions no molecular ion species or adduct ions were detected for SEX; the ion of highest  $m/z$  corresponded to loss of  $NO_2$  or  $HNO_2$  from a molecular ion species. The findings of collision-induced dissociation experiments are also discussed.

## INTRODUCTION

The *N*-acetylnitramines 1-acetylhexahydro-3,5-dinitro-1,3,5-triazine (TAX) (**1a**) and 1-acetyloctahydro-3,5,7-trinitro-1,3,5,7-tetrazocine (SEX) (**2a**) are important byproducts of the manufacture of the nitramine munitions compounds RDX (**1b**) and HMX (**2b**). Mass spectra of the latter two compounds obtained under a wide variety of ionizing conditions have been reported over the past two decades, and have been summarized in a recent review.<sup>1</sup> The fragmentation pathways of **1b** and **2b** in electron impact (EI) and positive and negative chemical ionization (PCI and NCI) modes have been extensively documented by the high-resolution collision-induced dissociation (CID) study of Yinon *et al.*<sup>2</sup> Of particular significance in this study was the demonstration of the presence in both CI modes of positive and negative  $[M + NO_2]$  and  $[M + NO]$  adduct ions, which, in addition to the molecular ions, gave rise to series of fragments. For **1b** in the NCI mode adduct  $[M + NO_2]^-$  predominated; no ions in the region of the relative molecular mass were observed in their work<sup>2</sup> or in the later study of McLuckey *et al.*<sup>3</sup> It is also noteworthy that in EI mode  $[M + NO]^+$  adducts were observed, at relative abundances of 1%, for both **1b** and its recently reported methylene homologue **3**.<sup>4</sup>

This paper reports the mass spectral characteristics of *N*-acetylnitramines **1a** and **2a**, which have not been previously described. While fragmentations with N-N bond cleavage and ring cleavage with loss of  $CH_2N_2O_2$  moieties in a manner similar to the fully nitrated ana-

logues were observed, there were significant differences in the behavior of the acetyl compounds.



## EXPERIMENTAL

The instrument used was a Finnigan MAT TSQ-70B with a 20-kV dynode detector. Samples, synthesized according to published procedures,<sup>5,7</sup> were introduced by a direct exposure probe (DEP), which consisted of a rhenium filament inserted directly into the electron beam or reagent gas plasma in the source and heated rapidly to desorb the sample before decomposition

0030-493X/91/020105-04 \$05.00

© 1991 by John Wiley &amp; Sons, Ltd.

Received 2 August 1990

Revised manuscript received 22 October 1990

Accepted 23 October 1990

This document has been approved for public release and sale; its distribution is unlimited.

91 2 20 067

could take place. A filament current increase of 16–17 mA s<sup>-1</sup> corresponded to a temperature gradient of 16–17 °C s<sup>-1</sup> and resulted in clean desorption within 2–3 s. Instrument parameters in the EI and both CI modes (methane as reagent gas) were electron energy 70 eV, emission current 200 µA, dynode 5–6 kV, electrometer amplifier gain 10<sup>-4</sup> mA V<sup>-1</sup>, source temperature 80 °C and scan time 0.5 s. For the CID experiments argon was the collision gas at 10 V collision energy and 1 × 10<sup>-3</sup> Torr collision cell pressure (1 Torr = 133.3 Pa); under these conditions the vacuum manifold pressure was 1.0 × 10<sup>-5</sup>–1.3 × 10<sup>-5</sup> Torr and the electrometer amplifier gain was reduced to 10<sup>-5</sup>–10<sup>-6</sup> mA V<sup>-1</sup>.

## RESULTS AND DISCUSSION

### Electron impact

The EI mass spectra of **1a** and **2a** (Table 1) are noteworthy in that the respective protonated molecular ions at  $m/z$  220 and 294 were the only ions observed in those regions. Although the observation of protonated molecular ions in EI is by no means unprecedented<sup>8</sup> and is known to occur with amides,<sup>9</sup> it is unusual not to see the unprotonated species at all; normally it is the more abundant. Elevation of the source temperature to 150 °C markedly increased the relative abundances of the proton adducts, and again no unprotonated species were seen. No higher adduct ions were detected at either temperature; a relative intensity of 0.2% was the detection limit.

Fragmentation patterns of the protonated molecular ions observed on CID (Table 2) were dissimilar to the respective EI mass spectra (Table 1). A predominant fragmentation process observed on CID for both **1a** and **2a** was loss of CH<sub>2</sub>CO, both alone and in combination with other moieties; in addition, there were significant differences between the congeners. For **1a**, loss of CH<sub>2</sub>CO alone yielding the  $m/z$  178 ion clearly predominated, and the ion resulting from loss of CH<sub>2</sub>CO and NO ( $m/z$  116) was a relatively minor fragment. Other significant pathways included loss of CH<sub>2</sub>NNO<sub>2</sub> both in combination with CH<sub>2</sub>CO to give the  $m/z$  104 fragment and in combination with another CH<sub>2</sub>NNO<sub>2</sub> moiety to give the  $m/z$  72 fragment. For **2a**, three equally abundant fragments were observed, and loss of NO in addition to CH<sub>2</sub>CO became an important pathway. Thus, the ions of  $m/z$  252, 190 and 116 arose from the loss of CH<sub>2</sub>CO, of CH<sub>2</sub>CO and NO and of NO and 2CH<sub>2</sub>NNO<sub>2</sub>, respectively.

### Chemical ionization

The characteristics of **1a** and **2a** in the PCI mode were similar to each other; the protonated molecular ions were substantially more abundant than in the EI mode, as expected (Table 1). The only adducts observed for each compound were hydrocarbon adducts (e.g. [M + C<sub>2</sub>H<sub>5</sub>]<sup>+</sup>) due to association reactions with methane-derived ions. While the most abundant ion for **1a** ( $m/z$  146) represented the loss of a CH<sub>2</sub>NNO<sub>2</sub> moiety and the two most abundant for **2a** ( $m/z$  220 and 146) rep-

resented losses of one and two of the same moiety, ions corresponding to the loss of CH<sub>2</sub>CO from MH<sup>+</sup> ( $m/z$  178 for **1a** and  $m/z$  252 for **2a**) were also prominent for both congeners. Losses of both CH<sub>2</sub>CO and CH<sub>2</sub>NNO<sub>2</sub> were reflected in the appearance of ions at  $m/z$  104 for **1a** and  $m/z$  178 for **2a**. Ions corresponding to losses of both NO and CH<sub>2</sub>NNO<sub>2</sub> moieties, not apparent in the EI mode, were found at  $m/z$  116 for **1a** and at  $m/z$  190 and 116 (2CH<sub>2</sub>NNO<sub>2</sub>) for **2a**.

Daughter-ion spectra of the protonated molecular ions observed in the PCI mode for **1a** and **2a** (Table 2) showed characteristics in common with the daughter-ion spectra in the EI mode, but there were significant differences both in the identities of the predominating fragments and in their relative abundances. As a general observation, in the PCI mode the loss of CH<sub>2</sub>NNO<sub>2</sub> is at least equally important as the loss of CH<sub>2</sub>CO. Specifically, for **2a** three of the four most abundant PCI fragments, all due to loss of CH<sub>2</sub>NNO<sub>2</sub> or combinations thereof, were not seen as EI daughters. In order of decreasing relative abundance, these ions were  $m/z$  220 (loss of CH<sub>2</sub>NNO<sub>2</sub>),  $m/z$  146 (loss of 2CH<sub>2</sub>NNO<sub>2</sub>) and  $m/z$  178 (loss of CH<sub>2</sub>NNO<sub>2</sub> and CH<sub>2</sub>CO). Two of the three fragments predominating in the EI mode, which were due to the loss of CH<sub>2</sub>CO or combinations thereof, were greatly reduced in abundance as PCI daughters ( $m/z$  252 and 190). For **1a**, similar effects were seen in the relative abundances of the fragments corresponding to the loss of CH<sub>2</sub>NNO<sub>2</sub> and CH<sub>2</sub>CO ( $m/z$  146 and 178, respectively). The former increased markedly in abundance (11% in EI to 76% in PCI) whereas the latter decreased (from 100% to 91%).

In contrast to their similar PCI characteristics, **1a** and **2a** differed dramatically in their NCI spectra. For **1a**, adduct ions were a prominent feature (Table 1). The second most abundant ion (69%) was the [M + NO<sub>2</sub>] adduct ( $m/z$  265); [M + NO] ( $m/z$  249) and [M + H] ( $m/z$  220) adducts were also present at much lower abundances (2% and 3%, respectively). The most abundant ion,  $m/z$  173, corresponded to [M - NO<sub>2</sub>]. On the other hand, the NCI mass spectrum of **2a** was distinguished by the absence not only of adducts but of any molecular ion species at all. Prominent fragment ions were  $m/z$  247, corresponding to [M - NO<sub>2</sub>], and  $m/z$  200, corresponding to loss of HNO<sub>2</sub> in addition to NO<sub>2</sub>. The most abundant ion again was  $m/z$  173, which for **2a** corresponded to loss of the CH<sub>2</sub>NNO<sub>2</sub> and NO<sub>2</sub> moieties.

Attempts to obtain daughter-ion spectra of the  $m/z$  265 adduct of **1a** in NCI were unsuccessful, and even when the collision cell pressure was lowered to 1 × 10<sup>-4</sup> Torr and Q3 was scanned over the range  $m/z$  100–270, no ions including the parent adduct were detected. However, selected reaction monitoring experiments with single ions at 1 × 10<sup>-4</sup> Torr suggested that the ion at  $m/z$  173 was a daughter ion and that at  $m/z$  220 probably was not. The finding of  $m/z$  102 as the most abundant daughter of the  $m/z$  247 ion in the NCI of **2a** provides the first evidence that ring cleavage can take place with loss of CH<sub>2</sub>NCOCH<sub>3</sub> ( $m/z$  71) in addition to loss of CH<sub>2</sub>NNO<sub>2</sub> ( $m/z$  74) in fragmentations of *N*-acetylnitramines.

It should be mentioned that, except in the failed case of NCI daughters of  $m/z$  265, no attempts were made to

Table 1. Mass spectra of *N*-acetylnitramines<sup>a</sup>

Compound	EI	PCI	NCI
<b>1a</b>			265 [M + NO <sub>2</sub> ] <sup>+</sup> (69)
			249 [M + NO] <sup>+</sup> (2)
			220 [M + H] <sup>+</sup> (3)
	220 [M + H] <sup>+</sup> (5)	220 [M + H] <sup>+</sup> (41)	
		202 [M - OH] <sup>+</sup> (6)	
		186 <sup>b</sup> (5)	
		178 [MH - CH <sub>2</sub> CO] <sup>+</sup> (30)	
173 [M - NO <sub>2</sub> ] <sup>+</sup> (10)	174 [MH - NO <sub>2</sub> ] <sup>+</sup> (10)	173 [M - NO <sub>2</sub> ] <sup>+</sup> (100)	
146 [M - CH <sub>2</sub> NNO <sub>2</sub> ] <sup>+</sup> (5)	146 [MH - CH <sub>2</sub> NNO <sub>2</sub> ] <sup>+</sup> (100)		
131 [M - CH <sub>2</sub> CO - NO <sub>2</sub> ] <sup>+</sup> (23)	132 [MH - CH <sub>2</sub> CO - NO <sub>2</sub> ] <sup>+</sup> (12)	129 <sup>b</sup> (50)	
99 [M - CH <sub>2</sub> NNO <sub>2</sub> - NO <sub>2</sub> ] <sup>+</sup> (100)	116 [MH - CH <sub>2</sub> NNO <sub>2</sub> - NO] <sup>+</sup> (3)		
<b>2a</b>	294 [M + H] <sup>+</sup> (2)	294 [M + H] <sup>+</sup> (9)	
	251 [M - CH <sub>2</sub> CO] <sup>+</sup> (4)	252 [M - CH <sub>2</sub> CO] <sup>+</sup> (16)	247 [M - NO <sub>2</sub> ] <sup>+</sup> (20)
	220 [MH - CH <sub>2</sub> NNO <sub>2</sub> ] <sup>+</sup> (8)	220 [MH - CH <sub>2</sub> NNO <sub>2</sub> ] <sup>+</sup> (95)	
	205 [M - CH <sub>2</sub> CO - NO <sub>2</sub> ] <sup>+</sup> (9)		
	201 [M - 2NO <sub>2</sub> ] <sup>+</sup> (14)	190 [MH - CH <sub>2</sub> NNO <sub>2</sub> - NO] <sup>+</sup> (9)	200 [M - NO <sub>2</sub> - HNO <sub>2</sub> ] <sup>+</sup> (22)
	178 [MH - CH <sub>2</sub> NNO <sub>2</sub> - CH <sub>2</sub> CO] <sup>+</sup> (79)	178 [MH - CH <sub>2</sub> NNO <sub>2</sub> - CH <sub>2</sub> CO] <sup>+</sup> (23)	
	173 [M - CH <sub>2</sub> NNO <sub>2</sub> - NO <sub>2</sub> ] <sup>+</sup> (23)	174 [MH - CH <sub>2</sub> NNO <sub>2</sub> - NO <sub>2</sub> ] <sup>+</sup> (31)	173 [M - NO <sub>2</sub> - CH <sub>2</sub> NNO <sub>2</sub> ] <sup>+</sup> (100)
	146 [MH - 2CH <sub>2</sub> NNO <sub>2</sub> ] <sup>+</sup> (100)	146 [MH - 2CH <sub>2</sub> NNO <sub>2</sub> ] <sup>+</sup> (100)	
	131 [M - CH <sub>2</sub> NNO <sub>2</sub> - CH <sub>2</sub> CO - NO <sub>2</sub> ] <sup>+</sup> (23)	132 [MH - CH <sub>2</sub> NNO <sub>2</sub> - CH <sub>2</sub> CO - NO <sub>2</sub> ] <sup>+</sup> (11)	129 <sup>b</sup> (5)
	99 [M - 2CH <sub>2</sub> NNO <sub>2</sub> - NO <sub>2</sub> ] <sup>+</sup> (96)	116 [MH - CH <sub>2</sub> NNO <sub>2</sub> - NO] <sup>+</sup> (40)	102 [M - NO <sub>2</sub> - CH <sub>2</sub> NNO <sub>2</sub> - CH <sub>2</sub> NCOCH <sub>3</sub> ] <sup>+</sup> (6)

<sup>a</sup> Relative abundances (%) are given in parentheses following the *m/z* values and structural assignments.

<sup>b</sup> No assignment

Table 2. CID daughter ions of *N*-acetylnitramines

Compound	Parent (P)	Daughters	Relative abundance (%)	
			EI	CI
<b>1a</b>	220	178 [P - CH <sub>2</sub> CO] <sup>+</sup>	100	91
		146 [P - CH <sub>2</sub> NNO <sub>2</sub> ] <sup>+</sup>	11	76
		116 [P - CH <sub>2</sub> NNO <sub>2</sub> - NO] <sup>+</sup>	6	5
		104 [P - CH <sub>2</sub> NNO <sub>2</sub> - CH <sub>2</sub> CO] <sup>+</sup>	42	100
		72 [P - 2CH <sub>2</sub> NNO <sub>2</sub> ] <sup>+</sup>	53	— <sup>a</sup>
<b>2a</b>	294	252 [P - CH <sub>2</sub> CO] <sup>+</sup>	91	36
		220 [P - CH <sub>2</sub> NNO <sub>2</sub> ] <sup>+</sup>	— <sup>b</sup>	67
		190 [P - CH <sub>2</sub> NNO <sub>2</sub> - NO] <sup>+</sup>	100	25
		178 [P - CH <sub>2</sub> NNO <sub>2</sub> - CH <sub>2</sub> CO] <sup>+</sup>	— <sup>b</sup>	39
		146 [P - 2CH <sub>2</sub> NNO <sub>2</sub> ] <sup>+</sup>	— <sup>b</sup>	43
		116 [P - 2CH <sub>2</sub> NNO <sub>2</sub> - NO] <sup>+</sup>	93	100
		104 [P - 2CH <sub>2</sub> NNO <sub>2</sub> - CH <sub>2</sub> CO] <sup>+</sup>	— <sup>b</sup>	9
	102 <sup>c</sup>	15	23	
	247	173 [P - CH <sub>2</sub> NNO <sub>2</sub> ] <sup>+</sup>	—	26
		102 [P - CH <sub>2</sub> NNO <sub>2</sub> - CH <sub>2</sub> NCOCH <sub>3</sub> ] <sup>+</sup>	—	100

<sup>a</sup> Not measured

<sup>b</sup> Not observed

<sup>c</sup> Fragmentation not assigned

optimize either the collision energy or the collision cell pressure. It has been demonstrated that fragmentation is more dependent on the latter than the former,<sup>10</sup> and the values were arbitrarily selected for this study.

## CONCLUSIONS

In contrast to the well documented EI characteristics of RDX,<sup>2</sup> HMX<sup>2</sup> and five other recently reported nitra-

mines,<sup>4</sup> proton adducts were the only molecular ion species observed for the *N*-acetylnitramines **1a** and **2a** in the EI mode. The fragmentation patterns of the proton adducts in CID experiments, in marked contrast to those of the molecular ions of other nitramines,<sup>4</sup> were largely or entirely different from the observed EI spectra. Fragments due to loss of NO<sub>2</sub> and CH<sub>2</sub>NNO<sub>2</sub> predominated in the EI spectra, whereas the protonated molecular ions gave largely fragments due to loss of CH<sub>2</sub>CO and, in the case of **2a**, NO.

PCI spectra of the *N*-acetylnitramines were similar; each showed the expected protonated molecular ions and no higher adducts. Ions resulting from loss of  $\text{NO}_2$ ,  $\text{NO}$  and  $\text{CH}_2\text{CO}$ , and also from ring cleavage, were abundant. CID fragmentation of the protonated molecular ions showed that ring cleavage with the loss of  $\text{CH}_2\text{NNO}_2$  was equally important as the loss of  $\text{CH}_2\text{CO}$ .

In the NCI mode, however, the characteristics of the *N*-acetylnitramines were completely different. For **1a**,

adduct ions were prominent and the  $[\text{M} + \text{NO}_2]$  adduct was the second most abundant in the spectrum. For **2a**, no adducts or molecular ion species were detected; the fragment of highest  $m/z$  (247) corresponded to the loss of  $\text{NO}_2$  or  $\text{HNO}_2$  from a molecular ion species. No such differences were seen in the NCI spectra of **1b** and **2b**.<sup>2</sup> Mass spectral investigations of other *N*-acetylnitramines are now in progress to determine whether these differences and others observed are general characteristics.

## REFERENCES

1. J. Yinon, *Forensic Mass Spectrometry*, pp. 105-130. CRC, Boca Raton, FL (1987).
2. J. Yinon, D. J. Harvan and J. R. Hass, *Org. Mass Spectrom.* **17**, 321 (1982).
3. S. A. McLuckey, G. L. Glish and P. E. Kelley, *Anal. Chem.* **59**, 1670 (1987).
4. J. Yinon, W. C. Brumley, G. M. Brilis and S. Bulusu, *Org. Mass Spectrom.* **25**, 14 (1990).
5. E. E. Gilbert, J. R. Leccacorvi and M. Warman, in *Industrial and Laboratory Nitrations*, ed by R. F. Gould, p. 337. ACS Symposium Series 22, American Chemical Society, Washington, DC (1976).
6. V. I. Siele, M. Warman, J. Leccacorvi, R. Hutchinson, R. Motto and E. E. Gilbert, *Alternative Processes for HMX Manufacture*. Technical Report ARLCO-TR-78008, U.S. Army Armament Research and Development Command, Dover, NJ, AD-A083793 (1979).
7. C. D. Bedford, B. D. Deas, M. M. Broussard and M. A. Geigel, *Preparation and Purification of Multigram Quantities of TAX and SEX*. Report, AD-A122816 (1982). Avail. NIST from Gov. Rep. Announce. Index (US) **83**, 1943 (1983).
8. A. G. Harrison, *Chemical Ionization Mass Spectrometry*, p. 15. CRC, Boca Raton, FL (1983).
9. F. W. McLafferty, *Interpretation of Mass Spectra*, 3rd ed., p. 223. University Science Books, Mill Valley, CA (1980).
10. H. Schweer, G. Mackert and H. W. Seyberth, *Biomed Environ. Mass Spectrom.* **19**, 94 (1990).

A-1 20